RESEARCH ARTICLE

Indoor Positioning Based on Bluetooth RSSI Mean Estimator for the Evacuation Supervision System Application

DARIUSZ JANCZAK[1], (Member, IEEE), **WOJCIECH WALENDZIUK**[1], **MACIEJ SADOWSKI**[1], **ANDRZEJ ZANKIEWICZ**[1], (Member, IEEE), **KRZYSZTOF KONOPKO**[1], **MACIEJ SLOWIK**[2], **AND MALGORZATA GULEWICZ**[2]

[1]Faculty of Electrical Engineering, Bialystok University of Technology, 15-351 Białystok, Poland
[2]Moose spolka z ograniczona odpowiedzialnoscia, 15-540 Białystok, Poland

Corresponding authors: Dariusz Janczak (d.janczak@pb.edu.pl) and Wojciech Walendziuk (w.walendziuk@pb.edu.pl)

ABSTRACT The novel approach to the Low Energy Bluetooth RSSI (Received Signal Strength Indicator) examination for a personal location during the evacuation process is presented in this paper. The presented system is based on stationary locating localization nodes installed inside the facility and portable wristbands worn by people. A method based on the propagation model and preliminary determination of its characteristics is used to calculate the wristband-locator distance. The accuracy of the distance estimations is increased by assuming Gaussian model of RSSI measurements and using the estimator of RSSI mean value. A modified multilateration approach is used to estimate the person's position in the 2D Cartesian coordinate system. The paper also includes the outcomes of experiments conducted on the proposed approach as it was applied to the prototype evacuation supervision system. The paper presents a comparison of the position estimation error for the proposed method based on the mean RSSI value estimator with the results obtained when raw RSSI values were used. Analysis and discussion of wristband position estimation error are also included.

INDEX TERMS Indoor navigation, indoor positioning systems, localization, smart buildings, Bluetooth Low Energy, received signal strength indicator, RSSI, safety devices.

I. INTRODUCTION

The necessity of determining the location of a given object employing electronic sources in real-time (RTLS – Real Time Location System) is one of the most frequently occurring problems in engineering projects. However, it may be solved if the following factors are considered: the conditions of the environment in which the object is located, the required accuracy of determining the location, or other requirements of the end user of the created solution [1], [2]. Nevertheless, in all cases of determining the location, the environmental

The associate editor coordinating the review of this manuscript and approving it for publication was Ze Ji.

conditions are significantly important [3]. They are connected with physical phenomena which differ in the case of the analysis of open space compared with the conditions inside buildings [4], [5].

In the case of the location of an object in the open space, GNSS (Global Navigation Satellite Systems) working within 1200 MHz and 1500 MHz frequency ranges is the most commonly used solution [1], [6]. The visibility of the proper number of satellites is the essential factor in the accurate estimation of the object location [7], [8]. In the case of closed spaces, e.g., residential or public buildings, this requirement is practically impossible to be met. Additionally, estimating the location in the vertical position, for example,

determining the floor in a building, is another important issue. The accuracy of determining the location in the vertical position, in the case of satellite navigation systems, is relatively low, which has been described in publications [9], [10]. It is also worth mentioning that, however, the GNSSs have been especially designed for estimating the location in open spaces, in the case of a building, devices working in WLAN/WSN (Wireless Local Area Network/Wireless Sensor Network) standards working in open bands (ISM) of the frequency of 2400 MHz, e.g., Wi-Fi or Bluetooth, are usually applied [11], [12]. Applying those standards for the purposes of location is possible but requires creating special algorithms providing this functionality, which are often based on advanced techniques of deep learning or fingerprint [13], [14], [15], [16], [17]. It is also possible to use systems working within other frequency ranges, e.g., 1400 MHz. However, these applications are only used for specific purposes, for example, remote vehicle controlling [18] or remote patient monitoring [19]. Moreover, radio frequency identification (RFID) systems, working within various frequency ranges, may also be used for the purpose of estimating location [20], [21], [22].

Applying the concept of the closest sensor [23], [24] is one of the simplest ways of estimating the location inside a building. It allows bounding a location to a certain sensor (receiver) on the basis of the value of the received signal. In this solution, the location of the object is identical to the location of the device which has received the highest level of the signal. The main advantage of this technique is the fact that it is easily implemented. However, it must be said that the receivers have to be placed quite densely in order to obtain the required accuracy, which significantly raises the cost of the system. Additionally, depending on the configuration of the corridors in the building, the location of the infrastructural elements and the users, it may happen that the higher level of the signal will be received by a quite distant device. This may be caused, for example, by the fact that closer stations were temporarily shaded. The 1-D type location system is an expansion of the concept of the closest sensor. In this solution, we assume the movement of the object only along one axis, and the position is estimated based on a proper algorithm. However, the location of the 2-D type (position on the plane) is a better and more accurate method, especially in the case of vast buildings. The 3-D type location (the location estimated according to three spatial coordinates) is rarely implemented, typical rather for open space estimations.

Because the signal from the located object usually does not contain information concerning its location, it is vital to determine the values that can be monitored and give a basis to estimate the location of the object. Here are the most frequently applied methods [25], [26], [27] in which this property is used:

- monitoring the level of the RSSI (Received Signal Strength Indicator), which shows the power level of the received radio signal. Based on the signal propagation loss, it is possible to determine the distance from the transmitter [28], [29], [30];
- the analysis of the transmitter-receiver signal time flow (Time of Arrival, ToA). This method requires applying time measurements of high accuracy [31], [32];
- analysis of time differences of signal arrivals from a transmitter to many receivers (Time Difference of Arrival, TDoA). When the location of at least two receivers and the time difference of the signal arrival are known, the object location can be estimated [33], [34];
- analysis of the angle of the signal arrival (Angle of Arrival, AoA). It is used in the case of UWB (Ultra Wideband) location systems [35], [36], [37], and it is based on locating the signal source with the use of the amplitude method and the amplitude-phase method. The necessity of using extended systems of antennas is undoubtedly a disadvantage of this solution;
- using the Doppler's method, i.e., the analysis of the transmitted and the received signal frequency, also called FDoA (Frequency Difference of Arrival). This method is mostly used in open spaces and moving objects [38], [39];
- hybrid methods which combine the above solutions, for example Doppler shift and AoA [40], Doppler shift and RSSI [41], TDoA, and AoA [42], ToA and RSSI [43] or AoA and RSSI [44];
- other ways of object locating, especially using data fusion [45], [46].

Among the above mentioned solutions, the RSSI method combined with the Bluetooth technology called BLE (Bluetooth Low Energy) is the cheapest and easiest to apply [47].

BLE technology is one of the most universal techniques using the transmission of information over short distances. Due to the high availability of electronic modules supporting this standard, low energy consumption and the possibility of using a smartphone (most have built-in BLE transceivers) to collect and process data, it has very high application potential. It can be used, for example, to monitor energy consumption in an intelligent building [48], monitor the presence of employees in an office [49], and in remote healthcare systems [50]. Applications in public safety management support systems (emergency management) are also possible [51]. Systems using the BLE standard also enable easy integration with artificial intelligence and machine learning methods [52].

The use of devices operating in the BLE standard requires prior calibration tests due to the possibility of signal dropouts in a real, non-uniform propagation environment. It requires prior calibration measurements due to the possibility of signal loss caused by the non-homogeneous environment [24]. This factor is often calibrated up to a certain power level, which is taken as 100% of the signal power. Its absolute value depends on the manufacturer of the device. Recently, numerous papers concerning estimating the location with the use of the RSSI factor have appeared [53], [54], [55]. Their authors usually

begin with a trial of analytical determining the signal level, and then try to measure the RSSI factor and estimate the location of a real object. In such cases, the multilateration technique is applied for this reason. It is based on the measurement of the RSSI signal value, the absolute time of the signal arrival from the transmitter to the remote ToA receiver, or the estimation of the differences in the signal arrival times at remotely located transmitting-receiving devices [16], [37].

One of the fields where information concerning object location inside a building is applied is the surveillance of technical buildings or surveillance of people within a certain area. It may also be the case of monitoring exhibits in museums [56], controlling children on buses [53], or evacuation supporting systems in public buildings [57].

This article contains an analysis of an electronic system supporting evacuation dedicated to residential homes. As they are inhabited by elderly people with various illnesses and disabilities, the certainty that all tenants have been evacuated in a dangerous situation is vital for their lives. It was assumed that the system would provide the monitoring of people's presence and would estimate their approximate location. If it appears that a person has not left the building, they may be helped, as their location is known. Such a system covers the area of a building and its closest environment. For systems of this type. i.e., installed inside a building, the following requirements may be assumed:

- a certain accuracy of location, depending on the end user's needs, e.g., a fire brigade requires not only information concerning the number of people in the building, but also looks for general information concerning the location of a person to be evacuated;
- scalability of the system by enabling adjusting subsequent elements such as locators and reference stations in other parts of the building;
- using cheap and easily accessible electronic components, transmitting-receiving devices and open-source telecommunication standards in order to provide the supply chain during the system commercialization phase;
- the low-energy factor of the system components, e.g., lowering the power level consumed by the transmitting-receiving modules, or switching them temporarily to the standby mode.

Those requirements are met by the presented location system. This paper also contains methods enabling the decrease of the numerical resources needed for estimating the location of an evacuated person. Due to this factor, quicker estimation of the position on the server with a minimized amount of the transferred data is possible.

A. OBJECTIVE AND CONTRIBUTIONS OF THE PAPER
The main purpose of the article was to develop methods of position estimation based on the RSSI level of the wristband Bluetooth signal received by stationary reference stations.

Moreover, the basic assumptions of the developed system were taken into account:

- cost minimization;
- the ability to handle a large number of supervised wristbands, which requires the development of position estimation algorithms with low computational requirements;
- ease and short installation time on a wide range of buildings, which excludes long-term tests at the installation site of a commercial system;
- reasonable requirements for the accuracy of location estimation.

In the designed evacuation surveillance system, a method using a propagation model and preliminary identification of its parameters was chosen for distance estimation. Another goal was to develop an algorithm for position estimation, which was designed based on a modified multilateration method.

The contribution of this paper to the research area includes:

- improving the accuracy of position estimation by using estimator of RSSI mean value and appropriate identification of the propagation model parameters;
- modification of multilateration algorithm for estimating the position of objects on a 2D plane, which take into account z coordinates of the locator nodes and the average wearing height of the wristband;
- confirmation of the performance efficiency of the worked-out methods through experimental tests, which were carried out in a prototype system for supervising the evacuation of people from a building.

Moreover, the paper presents the analysis of the average error in determining the x, y coordinates and discussion on estimator parameters and the locator nodes placement.

II. ESTIMATION OF 2D POSITION COORDINATES USING MULTILATERATION
The development of 2D location methods was the next stage of research carried out by authors on increasing the accuracy of location in the evacuation supervision system presented in [24]. This problem comes down to the determination of the Cartesian coordinates (x_1, y_1) of the location of the P_1 wristband (BLE transmitter) based on the knowledge of the coordinates (x_{Li}, y_{Li}) of the locator nodes (BLE receivers) and the distance d_i between the locators and the wristband. The idea of the issue is illustrated in Figure 1. In the case of 2D coordinates, an unambiguous solution can be obtained by processing distance measurements to at least three locator nodes. This is due to the fact that the case of using distances to two locator nodes leads to a solution that is satisfying for two points in the plane.

In the case of the evacuation monitoring system, the coordinates of the locators (x_{Li}, y_{Li}) are known from the measurements made at the installation stage. The distances d_i are estimated on the basis of RSSI measurements, which in the case of the implemented system is made based on a model of propagation losses, which describes the dependence of signal power on distance. Analyzing Figure 1, it can be
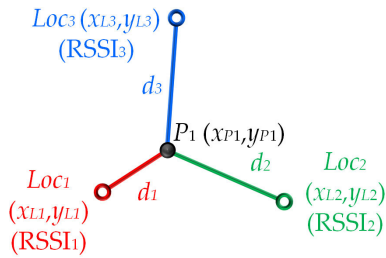
FIGURE 1. An example of system elements arrangement that allows to determine the 2D coordinates of an object based on RSSI.
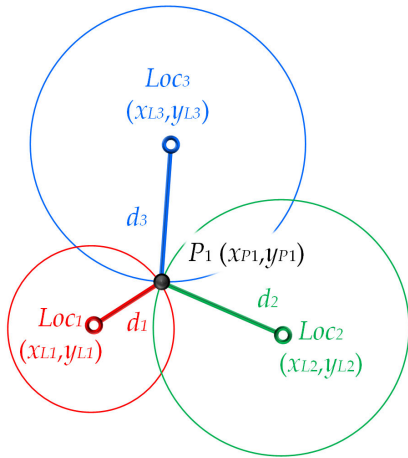

FIGURE 2. Determination of 2D coordinates of point $P1$ using circular multilateration.

FIGURE 3. Estimation of the 2D coordinates of point $P1$ using distance estimates $\hat{d}_i$.

to error.

$$\hat{d}_i(k) = d_i + v(k) \tag{2}$$

where $\hat{d}_i(k)$ is an estimate of the distance, $v(k)$ is the estimation error modeled as a normally distributed variable with zero mean and variance σ^2.

Therefore, circles usually do not intersect at a single point. For this reason, it impossible to obtain an analytical solution. It is illustrated in Figure 3. In this situation, to determine the coordinates $\left(x_{P_1}, y_{P_1}\right)$, a method to obtain an approximate solution [58], [60], such as the non-linear least squares method, the maximum likelihood estimator, or the estimation based on the centroid of the confidence area or the area formed by intersections of circles, should be used.

Additionally, it should be noted that in the case of an evacuation system, the located object is placed on the floor plane, which may allow the development of a simplified positioning algorithm.

These two issues discussed above were considered when developing the algorithm presented in the following sections.

III. ESTIMATION OF 2D POSITION COORDINATES USING MODIFIED 3D MULTILATERATION

It is assumed that in the designed evacuation supervision system, in the case of large rooms, the wristband should be seen by at least three locator nodes. Hence, the system of equations (1) should be formulated for $N \geq 3$ locator nodes obtaining RSSI measurements. In addition, it should be taken into account that the estimation of d_i distances based on the RSSI measurements and using the propagation loss model actually determine distances in the three-dimensional (3D) space. The height of the wristband placement (z coordinate) will usually be different from the installation height of the locator node. Not taking these facts into consideration when creating the mathematical description will lead to an increase in the error of the distance d_i estimation. Therefore, although the 2D coordinates of the wristband location are finally required, the system of equations (1) should be extended by the vertical z coordinate. Therefore, in order to determine the

observed that the accuracy of the estimation of the distance d_i (wristband - locator node distance) is the main factor affecting the accuracy of determining the (x_1, y_1) coordinates of point P_1. The solution to the given task can be obtained by using the multilateration methods [20], [58], [59].

Multilateration is one of the triangulation-based positioning methods. This method uses measurements of distances between the object and base stations with known locations. In the case of circular multilateration, the lines of the potential object location take the form of circles. The centers of the circles are located at the base stations, while the radius lengths of circles are obtained through the estimation of distances between the base stations and the object. This method is illustrated in Figure 2. As it can be seen in the figure, each two circles intersect at two points, and only the use of three circles unambiguously determines the location of object P_1 on the plane.

Using equations describing circles with centers at (x_{Li}, y_{Li}) and radii d_i for the system shown in Figure 2, the following system of equations can be formulated as follows:

$$\begin{aligned} (x - x_{L1})^2 + (y - y_{L1})^2 &= d_1^2 \\ (x - x_{L2})^2 + (y - y_{L2})^2 &= d_2^2 \\ (x - x_{L3})^2 + (y - y_{L3})^2 &= d_3^2 \end{aligned} \tag{1}$$

Solving the system of equations (1) leads to an unambiguous solution (x_{P1}, y_{P1}). Unfortunately, instead of the actual distances d_i, we have their estimates $\hat{d}_i(k)$ which are subject
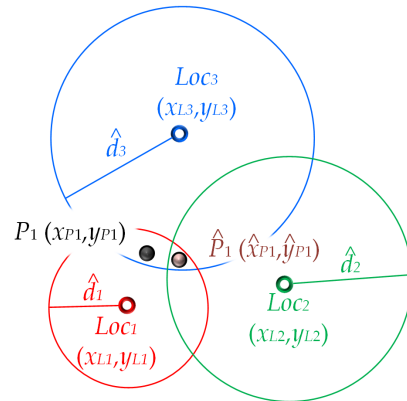
coordinates of the 2D location of point P_1 on the floor plane, a system of equations should be formulated for $N \geq 3$ spheres centered at points (x_{Li}, y_{Li}, z_{Li}) and radii d_i. Taking into account also the variability of the measurement process over time, the system of equations (1) takes the following form:

$$(x(k) - x_{L1})^2 + (y(k) - y_{L1})^2 + (z(k) - z_{L1})^2 = d_1^2(k)$$
$$(x(k) - x_{L2})^2 + (y(k) - y_{L2})^2 + (z(k) - z_{L2})^2 = d_2^2(k)$$
$$\vdots$$
$$(x(k) - x_{LN})^2 + (y(k) - y_{LN})^2 + (z(k) - z_{LN})^2 = d_N^2(k)$$
$$(3)$$

where $x(k)$, $y(k)$, $z(k)$ are the Cartesian coordinates of the wristband location (marked in Figure 2 as point P_1), x_{Li}, y_{Li}, z_{Li} are the Cartesian coordinates of the location of the locator nodes Loc_i, $d_i(k)$ are the distances between the wristband and the i-th locator node, k is the time index, N is the number of locator nodes in the system.

To reduce the order of the system of equations and simplify the calculations, the following approach is proposed. Taking into account the fact that the coordinates of the locator nodes installation are known and assuming the average height of wearing the wristband as $z(k) = z_o$, the dimension of space can be reduced. Therefore the system of equations (3) can be written in the form:

$$(x(k) - x_{L1})^2 + (y(k) - y_{L1})^2 = d_1^2(k) - (z_o - z_{L1})^2$$
$$(x(k) - x_{L2})^2 + (y(k) - y_{L2})^2 = d_2^2(k) - (z_o - z_{L2})^2$$
$$\vdots$$
$$(x(k) - x_{LN})^2 + (y(k) - y_{LN})^2 = d_N^2(k) - (z_o - z_{LN})^2$$
$$(4)$$

Expanding the above equations and subtracting the first equation from the others, the following system of equations can be obtained:

$$-2x_{L2}x(k) + 2x_{L1}x(k) + x_{L2}^2 - x_{L1}^2 - 2y_{L2}y(k)$$
$$+ 2y_{L1}y(k) + y_{L2}^2 - y_{L1}^2$$
$$= d_2^2(k) - d_1^2(k) + (z_{L1} - z_o)^2 - (z_{L2} - z_o)^2$$
$$\vdots$$
$$-2x_{LN}x(k) + 2x_{L1}x(k) + x_{LN}^2 - x_{L1}^2 - 2y_{LN}y(k)$$
$$+ 2y_{L1}y(k) + y_{LN}^2 - y_{L1}^2$$
$$= d_N^2(k) - d_1^2(k) + (z_{L1} - z_o)^2 - (z_{LN} - z_o)^2 \quad (5)$$

The system (5) can be written in matrix form as follows:

$$U \begin{bmatrix} x(k) \\ y(k) \end{bmatrix} = \frac{1}{2} V(k) \quad (6)$$

where

$$U = \begin{bmatrix} (x_{L2} - x_{L1}) & (y_{L2} - y_{L1}) \\ \vdots & \vdots \\ (x_{LN} - x_{L1}) & (y_{LN} - y_{L1}) \end{bmatrix}, \quad (7)$$

$$V(k) = \begin{bmatrix} x_{L2}^2 - x_{L1}^2 + y_{L2}^2 - y_{L1}^2 + (z_{L1} - z_o)^2 \\ - (z_{L2} - z_o)^2 + d_1^2(k) - d_2^2(k) \\ \vdots \\ x_{LN}^2 - x_{L1}^2 + y_{LN}^2 - y_{L1}^2 + (z_{L1} - z_o)^2 \\ - (z_{LN} - z_o)^2 + d_1^2(k) - d_N^2(k) \end{bmatrix} \quad (8)$$

The solution of (6) can be determined as follows [58], [59]:

$$\begin{bmatrix} \hat{x}(k) \\ \hat{y}(k) \end{bmatrix} = \frac{1}{2} \left(U^T U \right)^{-1} U^T V(k), \quad (9)$$

where $\hat{x}(k)$, $\hat{y}(k)$ are estimated values of the wristband coordinates.

Equation (9), together with (7) (8), allows obtaining estimates of Cartesian 2D coordinates of the wristband location, which take into account z_{Li} coordinates of the locator nodes and the average height of wearing the wristband. It should be emphasized that a low computational load characterizes the implementation of this algorithm. As it can be seen, the elements of the matrix U (7) depend only on the location coordinates of the locator nodes, so the matrix U is constant and can be calculated once. Therefore, the right part of the (9) can also be calculated once before the estimation process. The same can be done with most of the components of vector $V(k)$ (8). Such an approach greatly simplifies the computational process by reducing the algorithm for calculating estimates to the operation of multiplying a constant matrix by a vector, which significantly reduces the computational load. This is very important in a system working in real-time. However, in the case of real measurements, it must be considered that the wristband can be "seen" by different sets of locator nodes, which requires pre-calculation of the set of matrices U and elements of vectors $V(k)$ taking into account different combinations of locator nodes. However, in practice, the number of these sets will not be large, due to the limited wristband - locator node transmission range. With this approach, although the software implementing the estimator should be expanded with procedures for selecting the matrix U and the vector $V(k)$ from the pre-calculated set, the resulting computational load will be much smaller than in the case of calculating their values for each time moment k.

As it can be seen in (8), in order to obtain position estimate (9), it is necessary to determine the estimates of the distances between the wristband and the locator nodes. This issue is the subject of subsequent sections.

IV. RSSI-BASED DISTANCE ESTIMATION

As stated in Section II, the accuracy of determining the 2D position significantly depends on the quality of measurements of distances between the transmitter and locator nodes. The following two types of methods were investigated:

- with the use of a reference station;
- with the use of the initial identification of the parameters of the following model: $RSSI = f(d)$.

The method of distance estimation based on RSSI using a reference station is used in many studies presented in the

literature. In this case, the transmitter-receiver distance d is determined on the basis of the following model of function $RSSI = f(d)$ derived from the propagation relationship [55], [61], [62].

$$RSSI_d = RSSI_{d_0} + 20 \cdot \log_{10}\left(\frac{d}{d_0}\right), \qquad (10)$$

where d is the distance between the receiver and the transmitter, d_0 is the known distance to the reference station, while $RSSI_d$ and $RSSI_{d_0}$ are the RSSI values of the signal received from the transmitter being localized and the reference station.

After rearranging equation (10), the transmitter-receiver distance d estimate can be determined according to the following formula:

$$\hat{d} = 10^{\frac{RSSI_d - RSSI_{d_0}}{20}} \cdot d_0. \qquad (11)$$

In the case of the second method, which uses the initial identification of model parameters, the logarithmic model of the relationship $RSSI = f(d)$ is assumed in the following form [24]:

$$RSSI_d = a \cdot log10\,(d) + b, \qquad (12)$$

where d is the distance between the receiver and the transmitter, while a, b are parameters, the values of which depend on the type of system components, its surroundings and operating conditions.

The estimate of the distance d between the receiver and the transmitter, in this case, is determined according to the formula:

$$\hat{d} = 10^{\frac{RSSI_d - b}{a}}. \qquad (13)$$

The above method requires initial identification of parameters a, b of the model (12), which is carried out on the basis of a series of RSSI measurements of the signal received from transmitters located at points of known location.

In order to select one of the above methods to be used in the designed evacuation supervision system, an analysis of the advantages and disadvantages of each of them should be carried out. The analysis should take into account such features of the system as its spatial extent, reliability of measurements, immunity to interference and ease of installation. It can be presented as follows:

- The approach with the use of the reference station has the following advantages:
  - no need to conduct preliminary tests to identify system parameters;
  - immunity to changing environmental conditions when the entire system is subject to the same changes as the reference station.
- Disadvantages of the approach based on the use of the reference station:
  - the accuracy of the entire system depends on the stability of the RSSI measurements of the reference station, so a significant variance of the RSSI signal

of the reference station [24] will reduce the accuracy of measurements in the whole system;
  - local changes in the surroundings or conditions in which the reference station works cause a decrease in the accuracy of measurements in the entire system;
  - fragments of a large system operating in different conditions must have additional reference stations, which entails additional costs;
  - outlier RSSI [24] occurring in the measurements of reference station signal affects the obtained distance estimates in the entire system, causing a decrease in the accuracy of determining the position of objects in the system;
  - the use of transmitters from different manufacturers (other than the reference station) may cause an increase in distance estimation errors;
  - failure of the reference station causes malfunction of the entire system.

As it can be seen, in the case of a spatially extensive system, the approach based on the use of a reference station has numerous disadvantages. Therefore, in the designed evacuation supervision system, the method of estimating the distance between the location node and the wristband exploits equation (13) with pre-identification of model parameters in experimental research. The proposed approach does not require additional reference station devices and is free from disadvantages resulting from their use. It is expected that the measurement accuracy of the entire system will be comparable, but problems arising in the case of the reference station malfunction or changes in its operating conditions will be avoided.

Taking into account the above analysis, the RSSI-based estimate of the distance $d_{m,n}$ between the wristband located in the P_n position and the locator node Loc_m is determined according to (13). The estimate at the k-th time moment is calculated as follows:

$$\hat{d}_{im,n}\,(k) = 10^{\frac{RSSI_{m,n}(k) - b}{a}}, \qquad (14)$$

where $RSSI_{m,n}\,(k)$ is the RSSI of the signal transmitted by the wristband located in the P_n position and received by Loc_m locator node, $\hat{d}_{im,n}\,(k)$ is distance estimate, while a, b are parameters of the model which should be predetermined for each type of transmitter-receiver pair.

V. DISTANCE ESTIMATION WITH USING RSSI MEAN ESTIMATOR

In the case of indoor positioning systems based on the RSSI of the Bluetooth signal, a detailed analysis of error sources and their modeling is a complex issue that is described in the literature for idealized or simplified conditions. The complexity of this issue forces the adoption of approximate and generalized methods in systems implemented in practice. The method proposed in the article falls within this area. According to previous research carried out by the authors and presented in [24], the $RSSI_{m,n}\,(k)$ signal is stochastic, which

results from various types of disturbances and distortions related to the architecture of the building, various obstacles and interferences from other communication systems. Thus, the mean value and standard deviation of this stochastic process depend not only on the object location but also on its surroundings. This research leads to the use of a Gaussian RSSI model, which is a reasonably useful approximation. In this case, the distance estimation (14) is made not on the basis of current RSSI measurement ($RSSI_{m,n}(k)$), but on the basis of the estimated mean value of RSSI, hereinafter referred to as $RSSI_{m,n}^M(k)$. As an estimator of the mean RSSI value, it is proposed to use an averaging filter. The value of $RSSI_{m,n}^M(k)$ is obtained as following:

$$RSSI_{m,n}^M(k) = \frac{1}{M} \sum_{i=0}^{M-1} RSSI_{m,n}(k-i), \quad (15)$$

where M is the width of the moving window, and k is the index of the current time moment.

Finally, the distance estimation formula (14) will take the following form:

$$\hat{d}_{m,n}(k) = 10^{\frac{RSSI_{m,n}^M(k)-b}{a}}. \quad (16)$$

As mentioned above, parameters a, b should be predetermined for the types of system components (wristband, locator node) applied in the evacuation monitoring system. Identification of parameters a, b is carried out based on RSSI measurements obtained from wristbands placed in a number of known locations. Next, for all series of measurements carried out by each locator node for all wristband positions P_n the average of RSSI mean estimates values (denoted as $mRSSI_{m,n}$) should be calculated according to formula (17).

$$mRSSI_{m,n} = \frac{1}{N_{mn}} \sum_{i=1}^{N_{mn}} RSSI_{m,n}^M(i), \quad (17)$$

where $RSSI_{m,n}^M(i)$ is the i-th estimate of the RSSI mean obtained according to (15) for the signal transmitted by the wristband located in the P_n position and received by Loc_m locator node, N_{nm} is the number of RSSI measurements acquired by Loc_m locator node for each P_n wristband position.

Then, the parameters a, b of the model can be identified using the non-linear method of least squares. The applied logarithmic model (12) takes the following form:

$$mRSSI_{m,n} = a \cdot log_{10}(d_{m,n}) + b, \quad (18)$$

where $d_{m,n}$ is the real distance between the wristband located in the P_n position and the locator node Loc_m.

As it was shown in [24], a high level of RSSI signal variance is noticeable when the locator node operates under difficult conditions (like small space, the presence of interference sources). As a result, this phenomenon will significantly increase the variance of the distance estimate (14) determined on the basis of the current RSSI value ($RSSI_{m,n}(k)$). Whereas, the use of the estimator (15) of the mean RSSI value will result in a $\sqrt{M}$ fold reduction of the RSSI variance used

to determine the distance (16), which in turn will result in an improvement in the quality of the estimates $\hat{d}_{m,n}(k)$.

The width of the moving window M is an important parameter that should be selected optimally. Its increase reduces the variance of the filtered value, but at the same time, it may have a negative influence on the dynamics of the position estimates. Therefore, it should be selected carefully, taking into account the surroundings of the locator nodes. The selection of the parameter M can be carried out taking into account the error of estimation of the distance or position, as well as the frequency of refreshing RSSI information. It is recommended to set this parameter considering the locator node operating in the worst conditions in the entire system. However, the best solution is to set individual values for each locator node.

The distance estimation algorithm presented in this section and the algorithm for determining 2D coordinates presented in Section III were used to develop the evacuation supervision system. The experimental installation of this system is described in Section VI, and the results of the tests of the system are presented in Section VII.

VI. EVACUATION SUPERVISION EXPERIMENTAL SYSTEM

The research presented in this paper was conducted using an experimental installation of an evacuation supervision system. The experimental installation made it possible to check the operation of the designed system and to assess the effectiveness of the proposed methods for determining the 2D location. Below, the elements of the system will be described and the location of the locator nodes and the evacuation path will be illustrated.

A. LOCATOR NODE MODULES AND WRISTBANDS USED IN THE SYSTEM

The two main hardware components in the developed system are the locator nodes and the wristbands, which are presented in Figure 4. The locator node devices are based on the modules with ESP32 chips which provide Bluetooth Low Energy and WLAN (Wi-Fi) connectivity. Additionally, the locator nodes are equipped with some peripheral elements like microswitches, RGB LEDs, buzzers and Li-Ion battery charge controllers. The locator nodes are running dedicated firmware whose main function is to create a bridge between the wristbands (with BLE interface) and the IP network (through Wi-Fi connection). In addition, the firmware manages input-output peripherals that signalize the locator node charging and the wristband states. The main function of the wristbands is to broadcast their unique IDs with information about the detected heart pulse and movements of the person wearing them. The wristbands are built on the basis of open programmable modules based on a Nordic Semiconductor nRF52832 system-on-Chip (SoC) with an Arm Cortex-M4 processor and a Bluetooth Low Energy Transceiver. They also contain a heart rate sensor, an MEMS accelerometer and an OLED (Organic Light-Emitting Diode) display that is used to provide watch functions and to present some system state data.
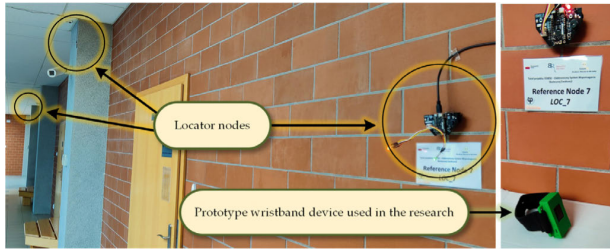
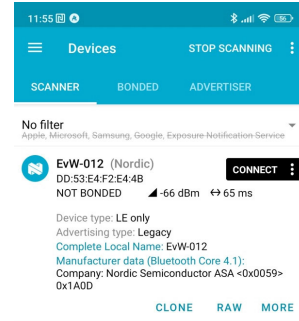**FIGURE 4.** General view of a part of the location system and a prototype wristband used in the research.

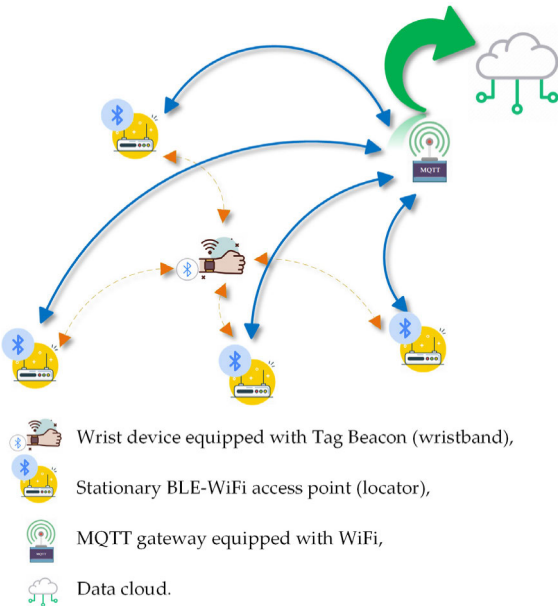**FIGURE 6.** Information reported by the wristband presented on the mobile application.

FIGURE 5. The functional structure of the evacuation supervision system.

B. EXPERIMENTAL SYSTEM

The functional structure of the evacuation supervision system is shown in Figure 5.

Dataflow of the evacuation supervision system presented in Figure 5 is organized in the following steps:

- The wristbands periodically broadcast BLE advertisements with a unique wristband ID and information about the detected pulse and movements of the wearer.
- The BLE advertisements (Figure 6) sent by the wristbands are received by the locator nodes that are in the range of the particular wristband. Then the locator node decodes the data from the received BLE advertisement and determines the signal level (RSSI). The locator node prepares a data frame with information from the wristband and sends it to the MQTT broker using a standard Wi-Fi Internet connection.
- A dedicated application running on the system server reads data from the MQTT broker and stores it in the system database. The software estimator module reads data from the database and uses it to perform the required estimation calculations. The estimation results are used by a dedicated web application to present them on the webpage.

The developed structure of the system allows for any scalability of the installation size of the evacuation supervision system. Depending on the extent of the building, its shape and room architecture, locator nodes can be added and arranged in any way. The only condition that must be met is their sufficiently dense distribution. Scalability is also of significant practical importance for the system, which should function in the event of a fire hazard. Scalability for this system also means that the system can function properly in the event of gradual degradation, which may occur when subsequent locator nodes are damaged due to, for example, fire. In the case of the developed architecture, the destruction of a certain number of them does not affect the efficiency of the rest of the system. However, in the "edge" case, i.e. the wristband is detected by only one or two locator nodes and multilateration is not possible, the system should switch to the proximity location described in the authors' article [24].

Experimental installation of the evacuation supervision system, working according to the presented scheme, was set up on the third floor of a university building, as shown in Figure 7. The system configuration, i.e. the location of the locator nodes, was planned in such a way that the tests were carried out on a potential evacuation path, and at the same time, the locator nodes were located in various interference conditions and different conditions of the multilateration geometry. Five locator nodes were placed on the walls of the lobby at the distances between 6 and 12 meters from each other. The coordinates of the locator nodes are shown in Table 1. The wristband was placed sequentially at 13 locations along the evacuation path. The coordinates of the wristband position nodes are shown in Table 2.

VII. RESULTS OF EXPERIMENTS

The developed algorithm for determining 2D coordinates using multilateration described in Sections III and V was verified using simulation and real data from RSSI measurements obtained in the experimental installation of the evacuation supervision system. At the beginning, comparative studies were carried out for the locator nodes and wristband locations arranged in accordance with the diagram shown in Figure 8. Then, the tests were carried out for the wristband placed along the evacuation path and with the use of all locators, as shown
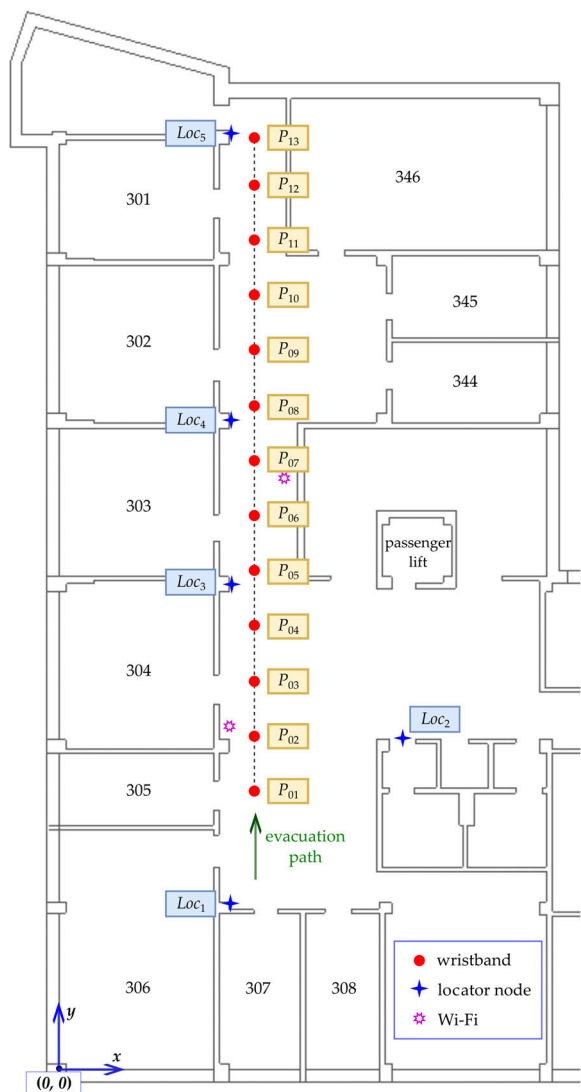
FIGURE 7. Location of Loc_m locator nodes in the experimental installation of the evacuation supervision system and locations P_n of wristband along the evacuation path during the tests.

TABLE 1. Coordinates of the locator nodes in the experimental installation of the evacuation supervision system.

Locator node	Coordinates
Loc_1	(6.26 6.32 2.74)
Loc_2	(12.41 12.22 2.74)
Loc_3	(6.26 18.24 2.74)
Loc_4	(6.26 24.17 2.74)
Loc_5	(6.26 34.47 2.74)

in Figure 7. The coordinates of the locator nodes and the wristband positions are presented in Tables 1 and 2.

A. SIMULATION RESEARCH OF THE ALGORITHM FOR DETERMINING 2D COORDINATES

Simulation tests were carried out in conditions corresponding to the measurement tests presented in the following sections, which allows the verification of the algorithm and software

TABLE 2. Coordinates of wristband placed along the evacuation path during the tests.

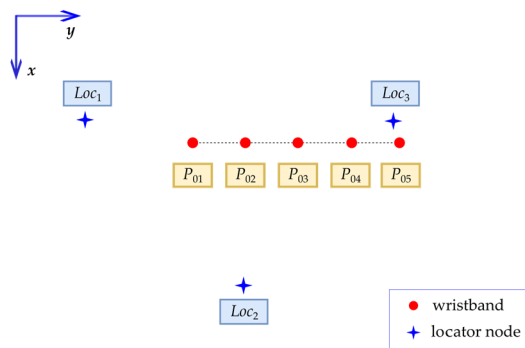| P_n	(x y z) [m m m]	P_n	(x y z) [m m m]	P_n	(x y z) [m m m]
P_{01}	(7.39 10.34 0.90)	P_{06}	(7.39 20.34 0.90)	P_{11}	(7.39 30.34 0.90)
P_{02}	(7.39 12.34 0.90)	P_{07}	(7.39 22.34 0.90)	P_{12}	(7.39 32.34 0.90)
P_{03}	(7.39 14.34 0.90)	P_{08}	(7.39 24.34 0.90)	P_{13}	(7.39 34.34 0.90)
P_{04}	(7.39 16.34 0.90)	P_{09}	(7.39 26.34 0.90)		
P_{05}	(7.39 18.34 0.90)	P_{10}	(7.39 28.34 0.90)		

FIGURE 8. Location of locator nodes and location of the wristband during simulation tests and a series of measurements.

and facilitates performance analysis and comparative tests. In the case of simulation studies, the distance measurement based on the RSSI was simulated in accordance with the measurement model with the additive Gaussian error most commonly found in the literature [61], [62]:

$$d_i^m(k) = d_i^r + v(k), \qquad (19)$$

where d_i^r is the real distance (in 3D space), $d_i^m(k)$ is a simulated distance measurement based on the RSSI at time moment k, while $v(k)$ is the measurement error modeled as an additive random process with normal distribution: $N[0, \sigma_d]$ (with zero mean and standard deviation σ_d).

Simulation tests for each of the wristband locations P_n were carried out in a series of $N_s = 500$ measurement simulations according to (19). Table 3 presents the values of the Mean Absolute Error (*MAE*) of the estimation of each of the coordinates (x, y) for six selected values of the standard deviation σ_d of the distance measurement error. The *MAE* value of each of the coordinates was determined according to the following formulas:

$$MAE(\hat{x}(k)) = \frac{1}{N_s} \sum_{k=1}^{N_s} \left| \hat{x}(k) - x_{P_n} \right|,$$

$$MAE(\hat{y}(k)) = \frac{1}{N_s} \sum_{k=1}^{N_s} \left| \hat{y}(k) - y_{P_n} \right|, \qquad (20)$$

where $\hat{x}(k)$, $\hat{y}(k)$ are estimates of the Cartesian coordinates of the wristband location, x_{P_n}, y_{P_n} are the actual Cartesian coordinates of the wristband position (P_n points), N_s is the number of RSSI measurements at a given wristband position.

TABLE 3. *MAE of the estimation of the coordinates (x, y) of the P_n points for different values of the standard deviation of the distance measurement error in the case of simulation research.*

	The standard deviation of distance measurement error: s_d [m]					
	1.0	2.0	3.0	5.0	10.0	20.0
P_{01}: $MAE(\hat{x}(k))$ [m]	1.11	2.17	3.29	5.88	14.73	44.67
P_{01}: $MAE(\hat{y}(k))$ [m]	0.62	1.25	1.82	3.32	7.51	21.83
P_{02}: $MAE(\hat{x}(k))$ [m]	1.05	2.08	3.33	5.60	14.63	39.96
P_{02}: $MAE(\hat{y}(k))$ [m]	0.60	1.15	1.69	3.01	7.49	19.68
P_{03}: $MAE(\hat{x}(k))$ [m]	1.13	2.21	3.38	5.74	14.04	42.05
P_{03}: $MAE(\hat{y}(k))$ [m]	0.63	1.23	1.85	2.93	7.56	19.98
P_{04}: $MAE(\hat{x}(k))$ [m]	1.30	2.65	3.92	6.59	16.11	43.06
P_{04}: $MAE(\hat{y}(k))$ [m]	0.71	1.38	2.05	3.52	8.42	20.80
P_{05}: $MAE(\hat{x}(k))$ [m]	1.61	3.09	4.71	7.46	18.27	48.00
P_{05}: $MAE(\hat{y}(k))$ [m]	0.79	1.55	2.47	4.10	8.76	24.09

As it can be seen from the results of the simulations presented in Table 3, the developed algorithm ((9) with (7), (8)) is characterized by good efficiency for a wide range of standard deviation values σ_d of the distance measurement errors. It enables the estimation of the coordinates (x, y) of the wristband position P_n with the *MAE* error at the level of the standard deviation value σ_d (for $\sigma_d < 5$ m). These values are satisfactory from the point of view of the evacuation supervision system. Differences between the estimation errors of the x coordinate and the y coordinate result from multilateration geometry and the location of points P_n relative to the location of locator nodes.

B. RESEARCH USING RSSI MEASUREMENTS IN THE EXPERIMENTAL EVACUATION SUPERVISION SYSTEM

The efficiency of the developed 2D coordinate estimation algorithm was checked for real RSSI measurements in the experimental evacuation supervision system. The locator nodes placement and the positions P_n of the wristband are presented in Section IV. Approximately $N_p = 500$ measurements were acquired for each P_n location.

First, it was necessary to identify the parameters *a, b* of the logarithmic model (12) of the relationship between the estimated RSSI mean value (15) and the transmitter-receiver distance *d* ($RSSI = f(d)$). The parameters a, b of the model were identified according to (17) and (18) using the non-linear method of least squares with the Levenberg-Marquardt algorithm.

Figure 9 illustrates the identification process of *a, b* parameters for $M = 10$, parameter of estimator (15). The blue dots on the graph, marked as $mRSSI_{m,n}$, represent the average values of the RSSI mean estimates obtained by the *m*-th locator node (Loc_m) of the signal from the wristband located in P_n position. The 3D distance between Loc_m and P_n is *d* meters. In the legend of the figure, the values of parameters *a, b* obtained in the identification process are given.
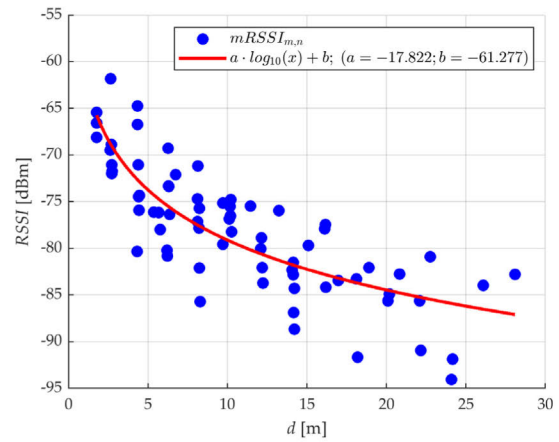

FIGURE 9. Identification of *a, b* parameters of the measurement model $RSSI = f(d)$ (for $M = 10$).

The identification process illustrated in Figure 9 was carried out for the Gaussian model of RSSI distribution. The values of $a = -17.822$, $b = -61.277$ were obtained, which minimized the mean square error of the fit. These values allow the estimation of the distance $\hat{d}_{m,n}(k)$ between Loc_m and P_n on the basis of the RSSI using (15) and (16).

Table 4 presents the standard deviations of distances estimated in this way for a series of RSSI measurements carried out in the experimental installation shown in Figure 7 by each of the three locator nodes (Loc_1, Loc_2, Loc_3) for the signal received from the wristband placed at selected points P_n (P_{01} - P_{05}). In order to demonstrate the efficiency of the proposed processing method (15), the table shows the results obtained from the raw RSSI values (marked as $M = 1$) and the results obtained with the application of the mean estimator (15) with a window width of $M = 10$.

As it can be seen in the results presented in Table 4, the standard deviation s_d of the estimated distances $\hat{d}_{m,n}(k)$, obtained based on RSSI using the proposed filter (15) with $M = 10$, ranges from approximately 0.1 m to values below 5 m. The obtained values are much lower than in the case of the estimated distances obtained with using raw RSSI values. The level of improvement obtained is in line with the theoretical predictions for this type of filter, which anticipates a decrease in the standard deviation by a factor of $\sqrt{M}$. The obtained reduction of the distance estimation error will allow improving the accuracy of the 2D estimation in the multilateration process and ultimately the improvement of the accuracy of the determined position. The obtained s_d values are within the range chosen during the simulation tests presented in Table 3, which enables the analysis of the effectiveness of the 2D algorithm, which are presented below.

During the research, it turned out that selection of the parameter M of the RSSI mean estimator (15) is an important parameter affecting the estimation error. This is illustrated in Figure 10, where the *MAE* of the distance estimates $\hat{d}_{m,n}(k)$ between Loc_m and P_n depending on the parameter M are presented. The *MAE* value of distance estimates was determined

TABLE 4. Standard deviations sd of distance estimates $\hat{d}_{m,n}(k)$ obtained from raw RSSI values (marked as $M = 1$) and using RSSI mean estimator (15) (window width $M = 10$).

	Loc_m	P_{01}	P_{02}	P_{03}	P_{04}	P_{05}
				s_d [m]		
	Loc_1	1.36	0.18	1.59	2.36	4.11
$M = 1$	Loc_2	2.30	5.04	1.39	5.37	5.73
	Loc_3	2.68	1.90	20.95	5.17	1.84
	Loc_1	0.50	0.06	0.51	0.76	1.13
$M = 10$	Loc_2	0.65	1.32	0.42	1.02	1.62
	Loc_3	0.83	0.68	4.68	0.69	0.47

according to the following formula:

$$MAE\left(\hat{d}_{m,n}(k)\right) = \frac{1}{N_s}\sum_{k=1}^{N_s}\left|\hat{d}_{m,n}(k) - d_{m,n}\right|, \quad (21)$$

where $d_{m,n}$ is the actual distance between Loc_m and P_n, while N_s is the number of RSSI measurements at a given wristband position.

As it can be seen in the graph presented in Figure 10, the *MAE* of distance estimation decreases with the increase of the window width M. These changes are significant for $M < 5$, while for $5 \leq M \leq 10$ are small. For $M > 10\ M$, the changes are insignificant. Taking into account the above results, it should be concluded that the value of M should be set between 5 and 10. In addition, the analysis of the graph presented in Figure 10 shows that for the recommended value of M, the *MAE* of distance estimation is approximately 30% lower when using the proposed RSSI mean estimator compared to using the raw RSSI values.

The study of the estimation efficiency of the proposed algorithms was carried out based on RSSI measurements obtained in the evacuation monitoring experimental system presented in Figure 7. For this purpose, the distance estimator (15), (16) and the 2D coordinate estimator (9) with (7), (8) were used. The average height of wearing the wristband was assumed as $z_o \approx 1.2$ m. An example of the coordinate estimation process is shown in Figure 11.

As shown in Figure 11, in the case of real data, the circles representing distances (estimated on the basis of RSSI mean estimates) from the locator nodes do not intersect at one point. The proposed position estimation method assumes the center of gravity of the common area as the point of the object location.

Table 5 presents the *MAE* of the $(x(k), y(k))$ coordinate estimates for wristbands located in the selected points P_n, based on measurements from Loc_1, Loc_2, Loc_3, for three window widths: $M \in \{3, 5, 10\}$ The table also includes the average position estimation error $\overline{b_{\hat{P}_n}}$, which was determined according to (22).

$$\overline{b_{\hat{P}_n}} = \frac{1}{N_s}\sum_{k=1}^{N_s}\sqrt{\left(\hat{x}(k) - x_{P_n}\right)^2 + \left(\hat{y}(k) - y_{P_n}\right)^2}, \quad (22)$$

where $\hat{x}(k)$, $\hat{y}(k)$ are estimates of the Cartesian coordinates of the wristband location, x_{P_n}, y_{P_n} are the actual Cartesian
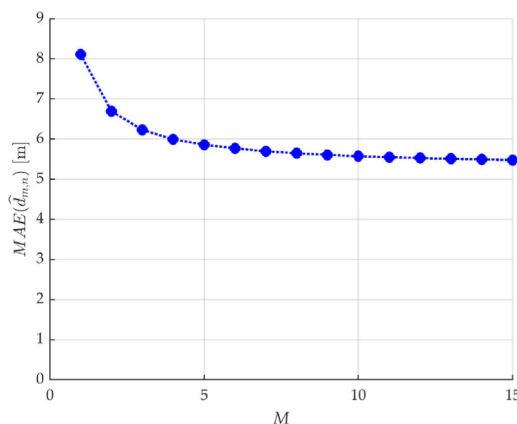

FIGURE 10. MAE of Loc_m - P_n distance estimation depending on the width of the window M.
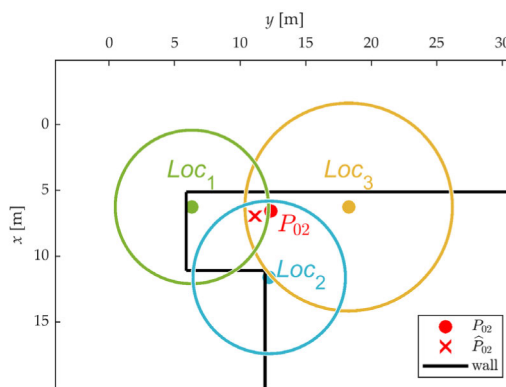

FIGURE 11. An example of the 2D coordinate estimation process in the experimental system based on the RSSI with the use of the proposed algorithms.

coordinates of the wristband position P_n, N_S is the number of RSSI measurements at a given wristband position.

From the data presented in Table 5, it can be concluded that the estimation errors decrease with the increase of the M value. As it can be seen, in the case of a change from $M = 3$ to $M = 10$, the decrease can be even twofold.

An example of a coordinate estimation process of $\hat{x}(k)$, $\hat{y}(k)$ for two sample points (P_{02}, P_{04}) is shown in Figure 12 and Figure 13. In the figures, the blue line indicates the estimates $\hat{x}(k)$, $\hat{y}(k)$, while the green line represents the actual value of the coordinate of the wristband location. The presented results were obtained for $M = 10$.

As shown in Figure 12 and Figure 13, the proposed estimator is characterized by a small error of the coordinates estimation, which has a value at the level of single meters. However, as it can be seen, a constant bias of some level may appear. The bias appearing for individual P_n locations results from the proposed method of identifying the model parameters. Its idea relies on the generalization of model parameters for the entire system. Therefore, the occurring bias can be reduced by identifying parameters a, b for each of the locator nodes separately or for a typical environment of a given group of locator nodes. However, this would require additional

TABLE 5. *MAE of the x, y coordinate estimates and average position estimation error* $\overline{b_{\widehat{P}_n}}$ *of selected* P_n *points based on measurements from:* $Loc_1, Loc_2, Loc_3,$ *for three M values.*

M		P_{01}	P_{02}	P_{03}	P_{04}	P_{05}
	$MAE(\hat{x}(k))$ [m]	6.65	3.69	3.53	2.38	5.61
$M = 3$	$MAE(\hat{y}(k))$ [m]	5.05	2.06	2.30	0.98	3.59
	$\overline{b_{\widehat{P}_n}}$ [m]	8.64	4.66	4.70	2.77	7.21
	$MAE(\hat{x}(k))$ [m]	4.67	3.12	3.03	1.78	4.61
$M = 5$	$MAE(\hat{y}(k))$ [m]	3.59	1.97	2.30	0.98	3.65
	$\overline{b_{\widehat{P}_n}}$ [m]	6.14	4.02	4.26	2.20	6.30
	$MAE(\hat{x}(k))$ [m]	3.12	2.77	2.50	1.41	4.03
$M = 10$	$MAE(\hat{y}(k))$ [m]	2.34	1.92	2.41	1.07	3.71
	$\overline{b_{\widehat{P}_n}}$ [m]	4.16	3.57	3.84	1.89	5.70

scaling tests during the installation of the system on target facilities. On the other hand, the bias level is acceptable from the point of view of accuracy required in the evacuation supervision system, which does not justify the additional effort during system installation. In addition, as it can be seen from the figures, there are single estimates $\hat{x}(k), \hat{y}(k)$ with a higher error level than the average. Although their level is also acceptable, their impact can be further mitigated by using an additional tracking algorithm with non-uniform sampling and outlier elimination [63], [64], [65], [66].

Table 6 presents the *MAE* of $(x(k), y(k))$ coordinate estimates for individual wristband locations P_n obtained based on RSSI mean estimates for measurements carried out in the experimental installation of the evacuation supervision system. The table also shows the average position estimation error $\overline{b_{\widehat{P}_n}}$, which was determined according to (22). The presented results were obtained for $M = 10$. Moreover, the average position estimation error $\overline{b_{\widehat{P}_o}}$ and *MAE* of coordinate $(x(k), y(k))$ estimates calculated for all measurements (all locations P_{01}-P_{13}) are presented in Table 7. For comparison, Table 8 presents the $\overline{b_{\widehat{P}_o}}$ and *MAE* obtained when raw RSSI values were used for distance estimates. Comparing these data with the results from Table 7 will allow to assess the effectiveness of the proposed method based on the RSSI mean value estimator.

The average position estimation error $\overline{b_{\widehat{P}_o}}$ is determined according to (23), and the *MAE* of coordinate $(x(k), y(k))$ estimates are calculated similarly. The average position estimation error $\overline{b_{\widehat{P}_o}}$ is determined as follows:

$$\overline{b_{\widehat{P}_o}} = \frac{1}{N_{P_n}N_S} \sum_{n=1}^{N_{P_n}} \sum_{k=1}^{N_S} \sqrt{(\hat{x}_n(k) - x_n)^2 + (\hat{y}_n(k) - y_n)^2},$$

(23)

where $\hat{x}_n(k), \hat{y}_n(k)$ are estimates of the Cartesian coordinates of the wristband position, x_n, y_n are the actual Cartesian coordinates of the wristband position P_n, N_S is the number of RSSI measurements at a given wristband position P_n, while N_{P_n} is the number of wristband locations P_n.

As it can be seen in the results presented in Tables 6 and 7, the developed algorithm ((9) with (7), (8) and (15), (16))
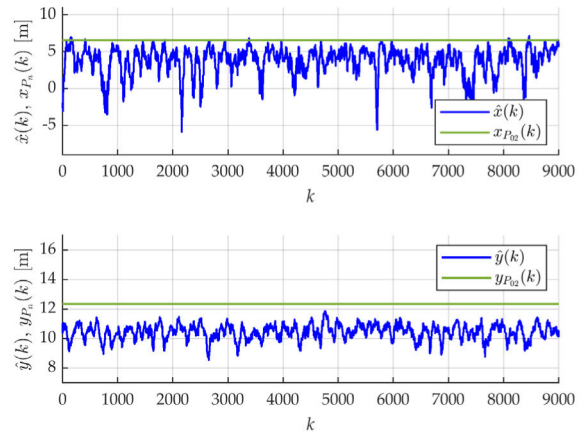

FIGURE 12. Estimation of the (x(k), y(k)) coordinates of the P_{02} point.
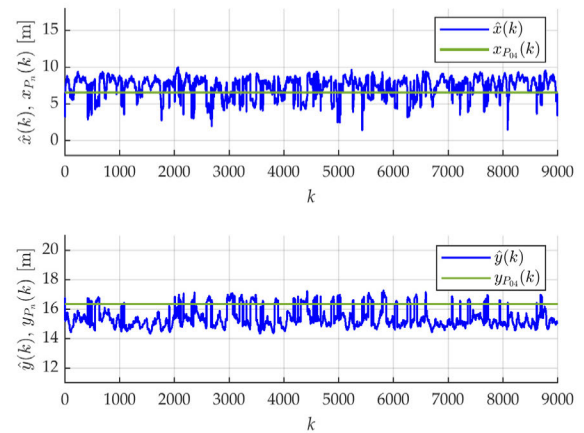

FIGURE 13. Estimation of the (x(k), y(k)) coordinates of the P_{04} point.

has a good efficiency. The accuracy analysis of the position estimation should be carried out for two separate areas on the evacuation path, i.e., points P_{01} - P_{07} and points P_{08} - P_{13}. Points P_{01} - P_{07} is in the close range ($d < 12$ m) of observations of the Loc_2 locator node, which results in smaller distance estimation errors. This ensures that the multilateration geometry in the x-axis direction is well-conditioned. Therefore, $MAE(\hat{x}(k))$ are at a low level, i.e., from about 1.5 m to about 4 m. On the other hand, points located further away from Loc_2 (P_{08} - P_{13}) are not observed with a low distance estimation error by the locator node spaced in the x-axis direction. It deteriorates conditioning of the multilateration geometry along the x-axis and causes an increase of $MAE(\hat{x}(k))$ even up to 19.6 m. The differences in the estimation accuracy of the y coordinate are much smaller, i.e., $MAE(\hat{y}(k))$ are from about 1 m to about 4 m for points P_{01} - P_{07} and from about 1 m to 9 m for points P_{08} - P_{13}. This is due to the fact that four locator nodes ($Loc_1, Loc_3, Loc_4, Loc_5$) are placed every 6 m to 12 m along the y axis (along the evacuation path), which ensures that the multilateration geometry in the y-axis direction is well-conditioned. The above analysis carried out for two ranges of points allows to formulate practical rules for the placement of the locator

TABLE 6. MAE of (x (k), y (k)) coordinate estimates and the average position estimation error $\overline{b_{\widehat{P_n}}}$ for individual wristband locations P_n.

P_n	$MAE(\hat{x}(k))$ [m]	$MAE(\hat{y}(k))$ [m]	$\overline{b_{\widehat{P_n}}}$ [m]
P_{01}	3.12	2.34	4.16
P_{02}	2.77	1.92	3.57
P_{03}	2.50	2.41	3.84
P_{04}	1.41	1.07	1.89
P_{05}	4.03	3.71	5.70
P_{06}	3.30	0.35	3.37
P_{07}	1.68	4.23	4.63
P_{08}	12.98	0.94	13.05
P_{09}	19.63	9.17	22.11
P_{10}	8.83	2.30	9.33
P_{11}	15.75	1.75	15.89
P_{12}	3.81	4.48	6.26
P_{13}	12.25	5.27	13.44

TABLE 7. MAE of (x (k), y (k)) coordinate estimates and the average position estimation error $\overline{b_{\widehat{P_o}}}$ for the proposed method based on mean rssi estimator.

	$MAE(\hat{x}(k))$ [m]	$MAE(\hat{y}(k))$ [m]	$\overline{b_{\widehat{P_o}}}$ [m]
$P01$-$P07$	2.67	2.25	3.83
$P01$-$P13$	6.73	2.98	7.85

TABLE 8. MAE of (x k), y k) coordinate estimates and the average position estimation error $\overline{b_{\widehat{P_o}}}$ obtained when raw rssi values were used.

	$MAE(\hat{x}(k))$ [m]	$MAE(\hat{y}(k))$ [m]	$\overline{b_{\widehat{P_o}}}$ [m]
$P01$-$P07$	7.80	3.29	9.15
$P01$-$P13$	11.89	4.74	13.68

nodes. In the case of large rooms, the locator nodes should be placed every 6 m to 12 m alternately on opposite walls of the hall. However, if the space where the wristband is located is in the form of a long corridor, it is acceptable to place the locator nodes along one wall. In this case, it is recommended to control the resulting estimates taking into account the location of the walls (the idea of the bounding box). As shown in Table 7, in the case of placing the locator nodes that enables good conditioning of the multilateration geometry, the average error in determining the x, y coordinates is about 2.5 m and the error $\overline{b_{\widehat{P_o}}}$ in determining the location of the wristband is about 3.8 m. In the case of ill-conditioned geometry, the average errors increase more than two times.

Comparison of results presented in Table 7 and Table 8 shows the effectiveness of the proposed method based on the RSSI mean value estimator. The use of this method resulted in a greater than 30% reduction in the MAE of the coordinate estimates and approximately a twofold reduction in the average position estimation error $\overline{b_{\widehat{P_o}}}$ compared to results of estimation when raw RSSI values were used.

In the test system, the estimator was implemented using Python v. 3.9.2 and was executed on a 64-bit ARM-8

Cortex-A53 1.2 GHz processor. For this implementation, the mean service time for one request (the time between receiving a message from the locator node and sending a message with the position estimate to the visualization module) equalled 9.64 ms. This time included not only determining the estimate but also parsing the received MQTT message and creating and sending an MQTT message to the visualization module. The resulting time enables the handling of over 100 messages per second, which ensures full functionality of the test system. Each wristband was uniquely identified in the system by its MAC address, so the measured RSSI and estimated distances from the locator were uniquely assigned to the wristband. During trials involving a group of a large number of people wearing wristbands, no problems were indicated. In the case of system expansion, the mean service time should be reduced, which can be achieved by using a larger number of estimators servicing groups of locator nodes, using a compiled programming language, or using a hardware platform with greater computing power.

VIII. CONCLUSION
The paper presents the developed methods for an indoor positioning system which is designed for an evacuation supervision system application. The designed system consists of a network of irregularly placed location nodes that receive signals from wristbands worn by people. To ensure low costs of installation, the system uses the Bluetooth RSSI values to locate the wristbands. In order to determine the position of a person in a 2D Cartesian coordinate system, a modified multilateration method was used. The proposed modification allows to take into account, in a 2D system, the z coordinates (height) of hanging the locators and the average height of wearing the wristband. This allows increasing the accuracy of the estimation while maintaining a low order of equations. However, the main advantage of the approach proposed in the paper is the increase in the accuracy of distance estimates used by the multilateration. This is achieved by using the mean RSSI value estimator instead of taking the raw RSSI values. To ensure a low computational load, an estimator in the form of an averaging filter was used. In the proposed approach, the process of identifying the parameters of the distance-RSSI exponential model is carried out on the basis of the estimated mean RSSI values. The proposed approach was verified during experiments carried out in a prototype evacuation supervision system. On these bases, recommendations concerning the choice of the M parameter of the RSSI mean estimator were concluded as $5 \le M \le 10$. Further research concerning the accuracy of the estimation of the wristband relocated along the evacuation path was conducted. On the basis of the completed tests, it appeared that the average estimation error value of the x, y coordinates was about 2.5 m, and the estimation error value of the wristband location was close to 3.8 m. The comparison of the position estimation error for the proposed method based on the mean RSSI value estimator with the results obtained when raw RSSI values were used showed an approximately two-fold error reduction.

The results show that the developed algorithm for determining 2D coordinates based on the RSSI mean estimator has satisfactory accuracy from the point of view of the evacuation surveillance system. Therefore, a target-tracking algorithm is not required. However, if necessary, such methods can be built on top of the proposed algorithm. In this case, for example, a linear Kalman filter could be applied using a dynamics model with a Newtonian transition matrix and a linear observation equation, where the estimates obtained using the method described in the article would be used as measurements. As other further research directions, we can mention the development of simplified methods for selecting the width M of the moving window depending on the conditions surrounding each locator, a method for optimizing the placement of locator nodes, and the use of data fusion with measurements from the IMU (Inertial Measurement Unit) module to improve the quality of position estimates of evacuated people.

Summarizing, thanks to its low computational requirements, the proposed solution allows its implementation in low-budget solutions based on Internet of Things technology.

REFERENCES

[1] R. S. Naser, M. C. Lam, F. Qamar, and B. B. Zaidan, "Smartphone-based indoor localization systems: A systematic literature review," *Electronics*, vol. 12, no. 8, p. 1814, Apr. 2023, doi: 10.3390/electronics12081814.

[2] Y. Zhuang, X. Sun, Y. Li, J. Huai, L. Hua, X. Yang, X. Cao, P. Zhang, Y. Cao, L. Qi, J. Yang, N. El-Bendary, N. El-Sheimy, J. Thompson, and R. Chen, "Multi-sensor integrated navigation/positioning systems using data fusion: From analytics-based to learning-based approaches," *Inf. Fusion*, vol. 95, pp. 62–90, Jul. 2023, doi: 10.1016/j.inffus.2023.01.025.

[3] A. Florio, G. Avitabile, and G. Coviello, "Geometric indoor radiolocation: History, trends and open issues," in *Machine Learning for Indoor Localization and Navigation*, S. Tiku and S. Pasricha, Eds. Cham, Switzerland: Springer, 2023, pp. 49–69, doi: 10.1007/978-3-031-26712-3_3.

[4] A. Sesyuk, S. Ioannou, and M. Raspopoulos, "A survey of 3D indoor localization systems and technologies," *Sensors*, vol. 22, no. 23, p. 9380, Dec. 2022, doi: 10.3390/s22239380.

[5] G. M. Mendoza-Silva, J. Torres-Sospedra, and J. Huerta, "A meta-review of indoor positioning systems," *Sensors*, vol. 19, no. 20, p. 4507, Oct. 2019, doi: 10.3390/s19204507.

[6] H. Xu, L.-T. Hsu, D. Lu, and B. Cai, "Sky visibility estimation based on GNSS satellite visibility: An approach of GNSS-based context awareness," *GPS Solutions*, vol. 24, no. 2, p. 59, Apr. 2020, doi: 10.1007/s10291-020-0973-5.

[7] M. Alghisi and L. Biagi, "Positioning with GNSS and 5G: Analysis of geometric accuracy in urban scenarios," *Sensors*, vol. 23, no. 4, p. 2181, Feb. 2023, doi: 10.3390/s23042181.

[8] A. Makar, "Limitations of multi-GNSS positioning of USV in area with high harbour infrastructure," *Electronics*, vol. 12, no. 3, p. 697, Jan. 2023, doi: 10.3390/electronics12030697.

[9] J. Lee, J. H. Kwon, and Y. Lee, "Analyzing precision and efficiency of global navigation satellite system-derived height determination for coastal and island areas," *Appl. Sci.*, vol. 11, no. 11, p. 5310, Jun. 2021, doi: 10.3390/app11115310.

[10] M. Specht, C. Specht, A. Stateczny, P. Burdziakowski, P. Dąbrowski, and O. Lewicka, "Study on the positioning accuracy of the GNSS/INS system supported by the RTK receiver for railway measurements," *Energies*, vol. 15, no. 11, p. 4094, Jun. 2022, doi: 10.3390/en15114094.

[11] Y. Zhuang, C. Zhang, J. Huai, Y. Li, L. Chen, and R. Chen, "Bluetooth localization technology: Principles, applications, and future trends," *IEEE Internet Things J.*, vol. 9, no. 23, pp. 23506–23524, Dec. 2022, doi: 10.1109/JIOT.2022.3203414.

[12] Y. Kwon and K. Kwon, "RSS ranging based indoor localization in ultra low power wireless network," *AEU-Int. J. Electron. Commun.*, vol. 104, pp. 108–118, May 2019, doi: 10.1016/j.aeue.2019.03.015.

[13] F. Kardas and Ö. Karal, "Wireless indoor localization problem with artificial neural network," in *Proc. Innov. Intell. Syst. Appl. Conf. (ASYU)*, Elazig, Turkey, Oct. 2021, pp. 1–5, doi: 10.1109/ASYU52992.2021.9599079.

[14] Y.-X. Ye, A.-N. Lu, M.-Y. You, K. Huang, and B. Jiang, "Wireless localization based on deep learning: State of art and challenges," *Math. Problems Eng.*, vol. 2020, pp. 1–8, Oct. 2020, doi: 10.1155/2020/5214920.

[15] V. Bellavista-Parent, J. Torres-Sospedra, and A. Pérez-Navarro, "Comprehensive analysis of applied machine learning in indoor positioning based on Wi-Fi: An extended systematic review," *Sensors*, vol. 22, no. 12, p. 4622, Jun. 2022, doi: 10.3390/s22124622.

[16] M. Petrović, M. Ciężkowski, S. Romaniuk, A. Wolniakowski, and Z. Miljković, "A novel hybrid NN-ABPE-based calibration method for improving accuracy of lateration positioning system," *Sensors*, vol. 21, no. 24, p. 8204, Dec. 2021, doi: 10.3390/s21248204.

[17] M. Petrovic, A. Wolniakowski, M. Ciezkowski, S. Romaniuk, and Z. Miljković, "Neural network-based calibration for accuracy improvement in lateration positioning system," in *Proc. Int. Conf. Mech. Syst. Mater. (MSM)*, Jul. 2020, pp. 1–6, doi: 10.1109/MSM49833.2020.9201646.

[18] M. Silarski and M. Nowakowski, "Performance of the SABAT neutron-based explosives detector integrated with an unmanned ground vehicle: A simulation study," *Sensors*, vol. 22, no. 24, p. 9996, Dec. 2022, doi: 10.3390/s22249996.

[19] A. Eshkevari and S. M. S. Sadough, "An improved method for localization of wireless capsule endoscope using direct position determination," *IEEE Access*, vol. 9, pp. 154563–154577, 2021, doi: 10.1109/ACCESS.2021.3128748.

[20] H. Obeidat, W. Shuaieb, O. Obeidat, and R. Abd-Alhameed, "A review of indoor localization techniques and wireless technologies," *Wireless Pers. Commun.*, vol. 119, no. 1, pp. 289–327, Jul. 2021, doi: 10.1007/s11277-021-08209-5.

[21] S. Cheng, S. Wang, W. Guan, H. Xu, and P. Li, "3DLRA: An RFID 3D indoor localization method based on deep learning," *Sensors*, vol. 20, no. 9, p. 2731, May 2020, doi: 10.3390/s20092731.

[22] A. Diallo, Z. Lu, and X. Zhao, "Wireless indoor localization using passive RFID tags," *Proc. Comput. Sci.*, vol. 155, pp. 210–217, Jan. 2019, doi: 10.1016/j.procs.2019.08.031.

[23] T. K. Geok, K. Z. Aung, M. S. Aung, M. T. Soe, A. Abdaziz, C. P. Liew, F. Hossain, C. P. Tso, and W. H. Yong, "Review of indoor positioning: Radio wave technology," *Appl. Sci.*, vol. 11, no. 1, p. 279, Dec. 2020, doi: 10.3390/app11010279.

[24] D. Janczak, W. Walendziuk, M. Sadowski, A. Zankiewicz, K. Konopko, and A. Idzkowski, "Accuracy analysis of the indoor location system based on Bluetooth low-energy RSSI measurements," *Energies*, vol. 15, no. 23, p. 8832, Nov. 2022, doi: 10.3390/en15238832.

[25] J. M. Kelner, C. Ziolkowski, L. Nowosielski, and M. Wnuk, "Localization of emission source in urban environment based on the Doppler effect," in *Proc. IEEE 83rd Veh. Technol. Conf. (VTC Spring)*, May 2016, pp. 1–5, doi: 10.1109/VTCSPRING.2016.7504324.

[26] S. Subedi and J.-Y. Pyun, "A survey of smartphone-based indoor positioning system using RF-based wireless technologies," *Sensors*, vol. 20, no. 24, p. 7230, Dec. 2020, doi: 10.3390/s20247230.

[27] I. Bisio, C. Garibotto, H. Haleem, F. Lavagetto, and A. Sciarrone, "On the localization of wireless targets: A drone surveillance perspective," *IEEE Netw.*, vol. 35, no. 5, pp. 249–255, Sep. 2021, doi: 10.1109/MNET.011.2000648.

[28] A. Poulose, J. Kim, and D. S. Han, "A sensor fusion framework for indoor localization using smartphone sensors and Wi-Fi RSSI measurements," *Appl. Sci.*, vol. 9, no. 20, p. 4379, Oct. 2019, doi: 10.3390/app9204379.

[29] J. Sangthong, J. Thongkam, and S. Promwong, "Indoor wireless sensor network localization using RSSI based weighting algorithm method," in *Proc. 6th Int. Conf. Eng., Appl. Sci. Technol. (ICEAST)*, Jul. 2020, pp. 1–4, doi: 10.1109/ICEAST50382.2020.9165300.

[30] D. J. Suroso, M. Arifin, and P. Cherntanomwong, "Distance-based indoor localization using empirical path loss model and RSSI in wireless sensor networks," *J. Robot. Control*, vol. 1, no. 6, pp. 199–207, 2020, doi: 10.18196/jrc.1638.

[31] X. Guo, Z. Chen, X. Hu, and X. Li, "Multi-source localization using time of arrival self-clustering method in wireless sensor networks," *IEEE Access*, vol. 7, pp. 82110–82121, 2019, doi: 10.1109/ACCESS.2019.2923771.

[32] Ç. Yapar, R. Levie, G. Kutyniok, and G. Caire, "Dataset of pathloss and ToA radio maps with localization application," 2022, *arXiv:2212.11777*.

[33] B. Ma, C. Tong, L. Zou, and M. Tian, "A TDOA localization method for complex environment localization," *J. Phys., Conf. Ser.*, vol. 2004, no. 1, Aug. 2021, Art. no. 012003, doi: 10.1088/1742-6596/2004/1/012003.

[34] Y. Zhao, Z. Li, B. Hao, and J. Shi, "Sensor selection for TDOA-based localization in wireless sensor networks with Non-Line-of-Sight condition," *IEEE Trans. Veh. Technol.*, vol. 68, no. 10, pp. 9935–9950, Oct. 2019, doi: 10.1109/TVT.2019.2936110.

[35] L. Barbieri, M. Brambilla, A. Trabattoni, S. Mervic, and M. Nicoli, "UWB localization in a smart factory: Augmentation methods and experimental assessment," *IEEE Trans. Instrum. Meas.*, vol. 70, pp. 1–18, 2021, doi: 10.1109/TIM.2021.3074403.

[36] N. Smaoui, M. Heydariaan, and O. Gnawail, "Single-antenna AoA estimation with UWB radios," in *Proc. IEEE Wireless Commun. Netw. Conf. (WCNC)*. Nanjing, China: IEEE, Mar. 2021, pp. 1–7, doi: 10.1109/WCNC49053.2021.9417526.

[37] M. Ciężkowski, S. Romaniuk, and A. Wolniakowski, "Apparent beacon position estimation for accuracy improvement in lateration positioning system," *Measurement*, vol. 153, Mar. 2020, Art. no. 107400, doi: 10.1016/j.measurement.2019.107400.

[38] S. Ferrand, F. Alouges, and M. Aussal, "A real-time indoor localization method with low-cost microwave Doppler radar sensors and particle filter," in *Computers Helping People With Special Needs* (Lecture Notes in Computer Science), vol. 12376, K. Miesenberger, R. Manduchi, and M. C. Rodriguez, Eds. Cham, Switzerland: Springer, 2020, pp. 467–474, doi: 10.1007/978-3-030-58796-3_54.

[39] A. Famili, A. Stavrou, H. Wang, and J. J. Park, "PILOT: High-precision indoor localization for autonomous drones," *IEEE Trans. Veh. Technol.*, vol. 72, no. 5, pp. 6445–6459, May 2023, doi: 10.1109/TVT.2022.3229628.

[40] K. Hao, Q. Xue, C. Li, and K. Yu, "A hybrid localization algorithm based on Doppler shift and AOA for an underwater mobile node," *IEEE Access*, vol. 8, pp. 181662–181673, 2020, doi: 10.1109/ACCESS.2020.3028608.

[41] I. S. Mohamad Hashim, A. Al-Hourani, and B. Ristic, "Satellite localization of IoT devices using signal strength and Doppler measurements," *IEEE Wireless Commun. Lett.*, vol. 11, no. 9, pp. 1910–1914, Sep. 2022, doi: 10.1109/LWC.2022.3187065.

[42] M. Aernouts, N. BniLam, R. Berkvens, and M. Weyn, "TDAoA: A combination of TDoA and AoA localization with LoRaWAN," *Internet Things*, vol. 11, Sep. 2020, Art. no. 100236, doi: 10.1016/j.iot.2020.100236.

[43] J. Kim, "Non-line-of-sight error mitigating algorithms for transmitter localization based on hybrid TOA/RSSI measurements," *Wireless Netw.*, vol. 26, no. 5, pp. 3629–3635, Jul. 2020, doi: 10.1007/s11276-020-02285-4.

[44] A. T. Le, L. C. Tran, X. Huang, C. Ritz, E. Dutkiewicz, S. L. Phung, A. Bouzerdoum, and D. Franklin, "Unbalanced hybrid AOA/RSSI localization for simplified wireless sensor networks," *Sensors*, vol. 20, no. 14, p. 3838, Jul. 2020, doi: 10.3390/s20143838.

[45] H. Mehrabian and R. Ravanmehr, "Sensor fusion for indoor positioning system through improved RSSI and PDR methods," *Future Gener. Comput. Syst.*, vol. 138, pp. 254–269, Jan. 2023, doi: 10.1016/j.future.2022.09.003.

[46] X. Dang, X. Si, Z. Hao, and Y. Huang, "A novel passive indoor localization method by fusion CSI amplitude and phase information," *Sensors*, vol. 19, no. 4, p. 875, Feb. 2019, doi: 10.3390/s19040875.

[47] J. Kunhoth, A. Karkar, S. Al-Maadeed, and A. Al-Ali, "Indoor positioning and wayfinding systems: A survey," *Hum.-Centric Comput. Inf. Sci.*, vol. 10, no. 1, p. 18, Dec. 2020, doi: 10.1186/s13673-020-00222-0.

[48] Z. D. Tekler, R. Low, C. Yuen, and L. Blessing, "Plug-mate: An IoT-based occupancy-driven plug load management system in smart buildings," *Building Environ.*, vol. 223, Sep. 2022, Art. no. 109472, doi: 10.1016/j.buildenv.2022.109472.

[49] Z. D. Tekler, R. Low, and L. Blessing, "An alternative approach to monitor occupancy using Bluetooth low energy technology in an office environment," *J. Phys., Conf. Ser.*, vol. 1343, no. 1, Nov. 2019, Art. no. 012116, doi: 10.1088/1742-6596/1343/1/012116.

[50] G. Alfian, M. Syafrudin, M. Ijaz, M. Syaekhoni, N. Fitriyani, and J. Rhee, "A personalized healthcare monitoring system for diabetic patients by utilizing BLE-based sensors and real-time data processing," *Sensors*, vol. 18, no. 7, p. 2183, Jul. 2018, doi: 10.3390/s18072183.

[51] A. Filippoupolitis, W. Oliff, and G. Loukas, "Occupancy detection for building emergency management using BLE beacons," in *Computer and Information Sciences* (Communications in Computer and Information Science), vol. 659. Cham, Switzerland: Springer, 2016, pp. 233–240, doi: 10.1007/978-3-319-47217-1_25.

[52] Z. D. Tekler, R. Low, B. Gunay, R. K. Andersen, and L. Blessing, "A scalable Bluetooth low energy approach to identify occupancy patterns and profiles in office spaces," *Building Environ.*, vol. 171, Mar. 2020, Art. no. 106681, doi: 10.1016/j.buildenv.2020.106681.

[53] S. Sakphrom, K. Suwannarat, R. Haiges, and K. Funsian, "A simplified and high accuracy algorithm of RSSI-based localization zoning for children tracking in-out the school buses using Bluetooth low energy beacon," *Informatics*, vol. 8, no. 4, p. 65, Sep. 2021, doi: 10.3390/informatics8040065.

[54] H. A. Hashim, S. L. Mohammed, and S. K. Gharghan, "Path loss model-based PSO for accurate distance estimation in indoor environments," *J. Commun.*, vol. 5, pp. 712–722, Feb. 2018, doi: 10.12720/jcm.13.12.712-722.

[55] X. Zhu and Y. Feng, "RSSI-based algorithm for indoor localization," *Commun. Netw.*, vol. 5, no. 2, pp. 37–42, 2013, doi: 10.4236/cn.2013.52b007.

[56] R. Giuliano, G. C. Cardarilli, C. Cesarini, L. Di Nunzio, F. Fallucchi, R. Fazzolari, F. Mazzenga, M. Re, and A. Vizzarri, "Indoor localization system based on Bluetooth low energy for museum applications," *Electronics*, vol. 9, no. 6, p. 1055, Jun. 2020, doi: 10.3390/electronics9061055.

[57] A. Depari, A. Flammini, D. Fogli, and P. Magrino, "Indoor localization for evacuation management in emergency scenarios," in *Proc. Workshop Metrol. Ind. 4.0 IoT*, Apr. 2018, pp. 146–150, doi: 10.1109/METROI4.2018.8428343.

[58] R. Zekavat and R. M. Buehrer, *Handbook of Position Location: Theory, Practice, and Advances*, vol. 8, 2nd ed. Hoboken, NJ, USA: Wiley, 2011.

[59] G. Li, E. Geng, Z. Ye, Y. Xu, and H. Zhu, "An indoor positioning algorithm based on RSSI real-time correction," in *Proc. 14th IEEE Int. Conf. Signal Process. (ICSP)*. Beijing, China: IEEE, Aug. 2018, pp. 129–133, doi: 10.1109/ICSP.2018.8652382.

[60] J. Yan, C. C. J. M. Tiberius, G. J. M. Janssen, P. J. G. Teunissen, and G. Bellusci, "Review of range-based positioning algorithms," *IEEE Aerosp. Electron. Syst. Mag.*, vol. 28, no. 8, pp. 2–27, Aug. 2013, doi: 10.1109/MAES.2013.6575420.

[61] B. Wang, S. Zhou, W. Liu, and Y. Mo, "Indoor localization based on curve fitting and location search using received signal strength," *IEEE Trans. Ind. Electron.*, vol. 62, no. 1, pp. 572–582, Jan. 2015, doi: 10.1109/TIE.2014.2327595.

[62] H. Zhou and J. Liu, "An enhanced RSSI-based framework for localization of Bluetooth devices," in *Proc. IEEE Int. Conf. Electro Inf. Technol. (EIT)*. Mankato, MN, USA: IEEE, May 2022, pp. 296–304, doi: 10.1109/eIT53891.2022.9813765.

[63] D. Janczak, M. Sankowski, and Y. Grishin, "Measurement fusion using maximum-likelihood estimation of ballistic trajectories," *IET Radar, Sonar Navigat.*, vol. 10, no. 5, pp. 834–843, Jun. 2016, doi: 10.1049/iet-rsn.2014.0316.

[64] Y. Bar-Shalom, X.-R. Li, and T. Kirubarajan, *Estimation With Applications to Tracking and Navigation*. New York, NY, USA: Wiley, 2001, doi: 10.1002/0471221279.

[65] Y. P. Grishin and D. Janczak, "A robust traclang fixed-lag smoothing algorithm in the presence of correlated outliers," in *Proc. Int. Radar Symp.* Wroclaw, Poland: IEEE, May 2008, pp. 1–4, doi: 10.1109/IRS.2008.4585755.

[66] M. Gupta, J. Gao, C. C. Aggarwal, and J. Han, "Outlier detection for temporal data: A survey," *IEEE Trans. Knowl. Data Eng.*, vol. 26, no. 9, pp. 2250–2267, Sep. 2014, doi: 10.1109/TKDE.2013.184.

DARIUSZ JANCZAK (Member, IEEE) received the M.Sc. degree in electrical engineering—automation and metrology and the Ph.D. degree in electrical engineering—signal processing from Bialystok University of Technology, Poland, in 1994 and 2002, respectively, and the Postdoctoral (Habilitation) degree in the scientific discipline of automation, electronics, and electrical engineering, in 2020. Since 1994, he has been with the Faculty of Electrical Engineering, Bialystok University of Technology, where he is currently an Assistant Professor. His research interests include signal processing, detection, and recognition of low probability of intercept signals, target tracking, navigation systems, data fusion, and fault detection and diagnosis.

WOJCIECH WALENDZIUK received the M.Sc. degree in electrical engineering—automation and metrology and the Ph.D. degree in electrical engineering from Bialystok University of Technology, Poland, in 1998 and 2007, respectively, and the Postdoctoral (Habilitation) degree in engineering and technical sciences in the scientific discipline of automation, electronics, and electrical engineering, in 2020. Since 2021, as an Associate Professor, he has been performing the function of the Head of the Department of Electrotechnics, Power Electronics and Electrical Power Engineering. He is a co-inventor of two granted patents and six patent applications and the author of more than 100 publications in the field of parallel processing, numerical methods, metrology, and measurement of nonelectrical quantities with the use of electrical methods. His main research interests include signal analysis, signal conditioners, and measurement systems application in medicine and unmanned aerial vehicles.

MACIEJ SADOWSKI received the M.Sc. degree in electronic and telecommunication engineering from Bialystok University of Technology, in 1996, and the Ph.D. degree in telecommunication from Wrocław University of Science and Technology, Poland, in 2004. He is currently with the Department of Photonics, Electronics and Lighting Technology, Faculty of Electrical Engineering, Bialystok University of Technology. He is the author/coauthor of more than 40 publications in the field of radiocommunications, antennas, electromagnetic compatibility, and measurement of electromagnetic fields. His main research interests include antennas and propagation, radiocommunication systems, the Internet of Things, and microwave technologies.

ANDRZEJ ZANKIEWICZ (Member, IEEE) received the M.Sc. degree in electronics and telecommunications and the Ph.D. degree in electrical engineering from Bialystok University of Technology, Poland, in 1996 and 2002, respectively. He is currently an Assistant Professor with the Department of Photonics, Electronics and Lighting Technology, Bialystok University of Technology. He supervised more than 100 master's and Engineering Diploma thesis. He is the author or coauthor of more than 50 publications mainly in the field of data transmission systems and digital signal processing. In his scientific and teaching activity he deals with data transmission networks, the IoT systems, problems of security of ICT systems, telecommunications systems, and digital signal processing issues. He serves as a peer reviewer in various international journals.

KRZYSZTOF KONOPKO received the M.Sc. degree in electronics and telecommunications and the Ph.D. degree in electrical engineering from Bialystok University of Technology, Poland, in 1998 and 2006, respectively. He is the author of more than 30 publications in the field of signal processing, parallel computing, and communication networks. His main research interests include wireless sensor networks, cognitive radio, and low probability intercept (LPI) signal detection and recognition.

MACIEJ SLOWIK received the M.Sc. degree in engineering from Bialystok University of Technology, in 2009, and the Ph.D. degree in automatics and robotics from the AGH University of Science and Technology, Poland, in 2018. He is Head of the Research and Development, main researcher and data scientist at Moose Inc. He is currently an engineer with overseeing projects at the intersection of ICT and robotics and the Internet of Things with more than ten years of experience successfully connecting world of industry and academia. He is also a scientist with a background in automation and robotics and unmanned aerial vehicles. He is currently involved in the development and use of Industry 4.0 and smart manufacturing in industry based on the Internet of Things technology, as well as data science and machine learning. He is a co-inventor of six patent applications and the author of 27 publications in the field of unmanned aerial vehicles, control systems, navigational systems, machine learning and applications of artificial intelligence, long short term memory artificial neural networks, and the Internet of Things.

MALGORZATA GULEWICZ received the L.L.M. degree from the University of Bialystok, in 2011. She is currently pursuing the Ph.D. degree with the Doctoral School, Faculty of Engineering Management, Bialystok University of Technology. Her thesis is connected with using IT technologies in the creation of digital twins for companies and processes. She is the Manager and the Product Owner with more than ten years of experience in information technologies, business development, project management, and product development. She is a co-owner and board member at Moose Inc. Her background includes projects in the areas of unmanned aerial vehicles, the Internet of Things, and digital twins. She is the author of six publications in the field of unmanned aerial vehicles, research and development projects, and digital twins. Her research interests include technology foresight and digital twins.

● ● ●